THE JOURNAL OF BIOLOGICAL CHEMISTRY VOL. 282, NO. 18, pp. 13895–13905, May 4, 2007

Structure and Conformational Changes in the C-terminal Domain of the β_2-Adrenoceptor

*INSIGHTS FROM FLUORESCENCE RESONANCE ENERGY TRANSFER STUDIES**

Received for publication, December 29, 2006, and in revised form, February 9, 2007 Published, JBC Papers in Press, March 8, 2007, DOI 10.1074/jbc.M611904200

Sébastien Granier[‡1], Samuel Kim[§], Aaron M. Shafer[‡], Venkata R. P. Ratnala[‡], Juan José Fung[‡], Richard N. Zare[§], and Brian Kobilka[‡2]

From the Departments of [‡]Molecular and Cellular Physiology and [§]Chemistry, Stanford University School of Medicine, Stanford, California 94305

The C terminus of the β_2-adrenoceptor (AR) interacts with G protein-coupled receptor kinases and arrestins in an agonist-dependent manner, suggesting that conformational changes induced by ligands in the transmembrane domains are transmitted to the C terminus. We used fluorescence resonance energy transfer (FRET) to examine ligand-induced structural changes in the distance between two positions on the β_2-AR C terminus and cysteine 265 (Cys-265) at the cytoplasmic end of transmembrane domain 6. The donor fluorophore FlAsH (Fluorescein Arsenical Helix binder) was attached to a CCPGCC motif introduced at position 351–356 in the proximal C terminus or at the distal C terminus. An acceptor fluorophore, Alexa Fluor 568, was attached to Cys-265. FRET analyses revealed that the average distances between Cys-265 and the proximal and distal FlAsH sites were 57 and 62 Å, respectively. These relatively large distances suggest that the C terminus is in an extended, relatively unstructured conformation. Nevertheless, we observed ligand-specific changes in FRET. All ligands induced an increase in FRET between the proximal C-terminal FlAsH site and Cys-265. Ligands that have been shown to induce arrestin-dependent ERK activation, including the catecholamine agonists and the inverse agonist ICI118551, led to a decrease in FRET between the distal FlAsH site and Cys-265, whereas other ligands had no effect or induced a small increase in FRET. Taken together the results provide new insight into the structure of the C terminus of the β_2-AR as well as ligand-induced conformational changes that may be relevant to arrestin-dependent regulation and signaling.

G protein-coupled receptors (GPCRs)[3] are versatile membrane proteins that regulate a wide variety of physiological functions. They respond to a large array of structurally diverse ligands and are the largest group of targets for drug discovery. Structure/function analysis has identified amino acids important for G protein coupling and ligand binding for several well characterized GPCRs, including the β-2 adrenoceptor (β_2-AR) (1). Moreover, many of these studies provide support for the accuracy of three-dimensional models of GPCRs based on the high resolution structure of bovine rhodopsin (2). However, few studies have directly addressed the mechanism by which diffusible ligands activate G protein-coupled receptors.

The most detailed information about structural changes associated with activation of a GPCR come from studies of rhodopsin. This is in part owing to its natural abundance and biochemical stability relative to other GPCRs. Electron paramagnetic resonance spectroscopy studies provide evidence that photoactivation of rhodopsin involves a rotation and tilting of transmembrane segment 6 (TM6) relative to TM3 (3). Light-induced conformational changes have also been observed in the cytoplasmic domain spanning TM1 and TM2, and the cytoplasmic end of TM7 (4–6).

Although rhodopsin has long been used as a model system for GPCR activation, it is unique among GPCRs because of the presence of a covalent linkage between the receptor and its ligand, retinal. Thus, the dynamic processes of agonist association and dissociation common to the GPCRs for hormones and neurotransmitters are not part of the activation mechanism of rhodopsin. The β_2-AR is activated by a functionally broad spectrum of diffusible ligands and is also a good model system to study the structural basis of ligand efficacy.

We have developed spectroscopic methods to characterize the structure of the β_2-AR and monitor ligand-induced conformational changes in real time (7–9). These studies provide evidence that agonists induce conformational changes in TM3 and TM6 of the β_2-AR that are similar to those observed upon activation of rhodopsin. We have obtained direct evidence that agonists and partial agonists induce distinct conformational states and that the process of agonist binding and activation occurs through at least two kinetically distinguishable conformational states (7–9).

* This work was supported by National Institutes of Health Grant R37NS28471 (to B. K.), National Science Foundation Grant BES-0508531 (to R. Z.), and the Mather's Charitable Foundation (to B. K.). The costs of publication of this article were defrayed in part by the payment of page charges. This article must therefore be hereby marked "*advertisement*" in accordance with 18 U.S.C. Section 1734 solely to indicate this fact.

[1] Supported by the Stanford Bio-X Graduate Student Fellowship and la Fondation pour la Recherche Médicale.

[2] To whom correspondence should be addressed: Dept. of Molecular and Cellular Physiology, Stanford University School of Medicine, Rm. B157 in Beckman Center, 279 Campus Dr., Stanford, CA 94305. Tel.: 650-723-7069; Fax: 650-498-5092; E-mail: kobilka@stanford.edu.

[3] The abbreviations used are: GPCR, G protein-coupled receptor; β_2-AR, β_2 adrenoceptor; TM, transmembrane domain; Tet-Gαs, membrane-tethered Gαs; FlAsH, Fluorescein Arsenical Helix or Hairpin binder; TCEP, Tris(2-carboxyethyl)phosphine; GRK, G protein-coupled receptor kinase; FRET, fluorescence resonance energy transfer; MAPK, mitogen-activated protein kinase; GTPγS, guanosine 5′-*O*-(thiotriphosphate); ERK, extracellular signal-regulated kinase.

Our previous studies have primarily focused on ligand-induced conformational changes in TM segments involved in ligand binding and G protein coupling. However, agonists induce changes in the receptor structure that promote phosphorylation of the C terminus by GPCR kinases (GRKs) and binding of arrestins (10, 11). These processes are important for receptor desensitization and agonist-induced internalization. Recent studies demonstrate that arrestin is also a signaling molecule (11, 12). Of interest, arrestin-dependent activation of ERK has been observed following activation by agonists and inverse agonists (13, 14), suggesting that the efficacy of ligands for guanine nucleotide binding protein Gs and arrestin signaling may differ.

The recent 2.2 Å crystal structure of rhodopsin reveals a structured C terminus folded over the 8th helix and the first cytoplasmic loop (15). However, this domain has relatively low homology with the C termini of other GPCRs. Moreover, the C terminus of the β_2-AR is 45 amino acids longer. It is therefore unlikely that they share the same structure.

To investigate the structure and ligand-induced conformational changes in this receptor domain, we have developed a FRET approach that allows us to monitor ligand-induced movement at two positions in the C terminus relative to the cytoplasmic end of TM6. The donor fluorophore FlAsH (Fluorescein Arsenical Helix binder) was attached to a CCPGCC motif introduced at position 351–356 in the proximal C terminus (10 residues after the palmitoylation site) or at the distal C terminus (after residue 413). The acceptor fluorophore Alexa Fluor 568 was introduced at a single reactive cysteine (Cys-265) at the cytoplasmic end of TM6. FRET analyses provided evidence that the C terminus is in an extended conformation; nevertheless, we observed ligand-specific effects on FRET between Cys-265 and the proximal and distal FlAsH sites. The results provide insights into structural features that may be relevant to interactions between the C terminus of the β_2-AR and regulatory proteins such as GRKs and arrestins.

EXPERIMENTAL PROCEDURES

Construction of the β_2-AR Mutants

The template used for site-directed mutagenesis was the human β_2-AR cDNA epitope tagged at the N terminus with the cleavable influenza-hemagglutinin signal sequence followed by the FLAG epitope and at the C terminus with 6 histidines. The mutations were generated on a background in which 4 of the 13 native cysteines in the receptor had been mutated as follows: C77V, C327S, C378A, and C406A. In this modified receptor (β_2-AR-Δ4 background), the only maleimide-reactive cysteine is Cys-265 (16). Mutations were all generated by polymerase chain reaction-mediated mutagenesis using *Pfu* polymerase according to the manufacturer's instructions (Stratagene, La Jolla, CA). The mutated cDNA was then digested with appropriate enzymes and cloned into pFastBac1 vector. All constructs were confirmed by restriction enzyme analysis and DNA sequencing.

Receptor Expression and Purification from Sf9 Insect Cells

Sf9 insect cells were grown at 27 °C in suspension cultures in ESF-921 medium (Expression Systems) supplemented with 0.5 mg/ml gentamicin. Recombinant baculoviruses were generated in Sf9 cells using the Bac-to-Bac® Baculovirus Expression System (Invitrogen). For receptor purification, Sf9 cell cultures at a density of $\sim 3 \times 10^6$ cells/ml were infected with appropriate viruses and harvested after 60 h by centrifugation (10 min at 5000 × *g*). The cell pellets were kept at −70 °C until used for purification.

Receptors were purified using a two-step purification procedure. Appropriate amounts of cell pellets were lysed in lysis buffer (10 mM Tris-HCl, pH 7.5, with 1 mM EDTA, 1 μM alprenolol, 160 μg/ml benzamidine, and 2.5 μg/ml leupeptin). Following centrifugation (20 min at 30,000 × *g*), the lysed cells were resuspended in solubilization buffer (20 mM Tris-HCl, pH 7.5, with 1.0% *n*-dodecyl-maltoside (DDM) (Anatrace), 100 mM NaCl, 160 μg/ml benzamidine, 2.5 μg/ml leupeptin and 1 μM alprenolol), subjected to 30 strokes of tight dounces using Wheaton dounce tissue grinder (Millville, NJ), and then stirred for 1 h at 4 °C. The solubilized receptor was purified by chromatography using M1 FLAG antibody affinity resin (Sigma). The eluate from the M1 anti-FLAG column was further purified on an alprenolol-Sepharose affinity column and finally through a second M1 FLAG antibody affinity resin purification step. Purified detergent-soluble receptor was stored in HLS buffer (20 mM Hepes, pH 7.5, 100 mM NaCl, and 0.1% DDM). The concentration of functional, purified receptor was determined as follows: purified receptor was incubated in triplicate in HLS buffer with a saturating concentration of [^{3}H]dihydroalprenol (10 nM) in a total volume of 100 μl for 1 h at room temperature. Free [^{3}H]dihydroalprenol was separated from bound by passing through a Sephadex G50 Medium column (4 × 0.5 cm). Nonspecific binding was determined in the presence of 1 μM alprenolol.

[^{35}S]GTPγS Binding

Purified β_2-AR and Tet-Gαs protein were mixed in a molar ratio of 1:5 and reconstituted as described previously (17). Briefly, reconstituted receptor (100 nM, final concentration) and Tet-Gαs were resuspended in 500 μl of cold binding buffer (75 mM Tris-HCl, pH 7.4, 12.5 mM $MgCl_2$, and 1 mM EDTA) supplemented with 0.05% (w/v) bovine serum albumin, 0.4 nM [^{35}S]GTPγS, and 1 μM GDP with or without β_2-AR ligands. Incubations were performed for 30 min at 25 °C with shaking at 230 rpm. Nonspecific binding was determined in the presence of 100 μM GTPγS and was always less than 0.2% of total binding. Bound [^{35}S]GTPγS was separated from free [^{35}S]GTPγS by filtration through glass fiber filters followed by three washes with 3 ml of cold binding buffer. Filter-bound radioactivity was determined by liquid scintillation counting.

Fluorescence Labeling of Purified Receptors

For double-labeled receptor, purified receptors (100 μl) were reacted overnight at 16 °C in the dark with 3 equivalents of FlAsH (commercially known as Lumio^{TM}Green labeling reagent) and Tris(2-carboxyethyl)phosphine (TCEP) (100 μM). Alexa Fluor 568 maleimide (1.1 equivalents) was then added to the mixture for 10 min at 4 °C.

For Alexa Fluor 568-labeled receptor, purified receptors (100 μl) were first incubated overnight at 16 °C in the dark in

the exact same conditions as for the double-labeled receptor but without FlAsH and without TCEP. Then, 1.1 equivalents of Alexa Fluor 568 maleimide were added to the mixture for 10 min at 4 °C. The fluorophore-labeled receptors were separated from the free dye by gel filtration on a desalting column equilibrated with a buffer containing 100 mM NaCl, 20 mM HEPES, pH 7.5, 0.1% dodecylmaltoside with 0.01% cholesterolhemisuccinate.

The donor/receptor and acceptor/donor ratio was determined by dividing the bound dye concentration (calculated by using the maximum absorbance of the donor- or acceptor-labeled receptor) by the donor or receptor concentration (determined by absorbance or ligand binding, respectively). The ratio of donor to receptor ranged from 0.8 to 1 dye/receptor. The typical acceptor/donor labeling ratios ranged from 1 to 1.3 (extinction coefficients $\epsilon_{\mathrm{FlAsH,528}} = 70{,}000\ \mathrm{cm^{-1}\,M^{-1}}$ and $\epsilon_{\mathrm{Alexa568,578}} = 91{,}300\ \mathrm{cm^{-1}\,M^{-1}}$).

Fluorescence Spectroscopy

General Conditions—Experiments were performed on a SPEX FluoroMax-3 spectrofluorometer with photon counting mode using an excitation and emission bandpass of 2 nm in S/R acquisition mode. Unless otherwise indicated, all experiments were performed at 25 °C. The final concentration of receptor used for spectroscopy ranged from 10 to 40 nM.

FRET Spectroscopy—For each FRET experiment, spectra were taken from receptor labeled with donor at FlAsH sites and acceptor at Cys-265 or receptor labeled with only the acceptor fluorophore at Cys-265. For each type of receptor, two types of emission scans were acquired. The first emission scan (donor scan) acquired used the excitation maximum for the donor fluorophore. The second emission scan (acceptor scan) used the excitation maximum for the acceptor fluorophore. The donor/acceptor pair used 508 nm excitation for the donor and 578 nm excitation for the acceptor. For testing the effects of β_2-AR-specific drugs, samples (±) drug were gently mixed and incubated for 15 min at room temperature. Three separate samples were used for testing each type of drug, and individual spectra were acquired and averaged. Drug concentrations varied from 10 μM to 1 mM. Emission spectra of the drugs in buffer were obtained at both the donor and acceptor excitation wavelengths and subtracted from the spectra obtained from the samples containing the receptor and drug (see below). Background fluorescence of the buffer was subtracted from spectra derived from the sample containing only the receptor. Removal of acceptor bleedthrough and correction of drug-induced acceptor fluorescence intensity changes were carried out and described in detail below.

Analysis of FRET Data

In this section, we use the following symbols to refer to the experimental emission spectra used for analysis, determined using the receptor with donor FlAsH on CCPGCC motif and acceptor Alexa Fluor 568 on Cys-265, or the receptor labeled only with acceptor on Cys-265, after excitation at the donor wavelength (ExcD) or at the acceptor wavelength (ExcA) as shown in Equation 1.

$$\begin{cases} A = \text{receptor labeled with donor and acceptor, ExcD} \\ A' = \text{receptor labeled with donor and acceptor, ExcA} \\ B = \text{receptor labeled with acceptor, ExcD} \\ B = \text{receptor labeled with acceptor, ExcA} \\ A_{\mathrm{drug}} = \text{same as } A\text{, with drug, ExcD} \\ A'_{\mathrm{drug}} = \text{same as } A'\text{, with drug, ExcA} \\ S_{\mathrm{buff}} = \text{buffer, ExcD} \\ S'_{\mathrm{buff}} = \text{buffer, ExcA} \\ S_{\mathrm{drug}} = \text{drug alone, in buffer, ExcD} \\ S'_{\mathrm{drug}} = \text{drug alone, in buffer, ExcA} \end{cases} \quad \text{(Eq. 1)}$$

Background fluorescence from either buffer or drug is removed as shown in Equation 2.

$$\begin{cases} C = A - S_{\mathrm{buff}} \\ C' = A' - S'_{\mathrm{buff}} \\ D = A_{\mathrm{drug}} - S_{\mathrm{drug}} \\ D' = A'_{\mathrm{drug}} - S'_{\mathrm{drug}} \\ E = B - S_{\mathrm{buff}} \\ E' = B' - S_{\mathrm{buff}} \end{cases} \quad \text{(Eq. 2)}$$

In spectrum E, the only signal is from direct excitation of the acceptor at ExcD. In spectra C and D, the signal from direct excitation of the acceptor is mixed with donor and FRET signals. However, the contribution from direct excitation of the acceptor in spectrum C and D is proportional to spectrum E, with a scaling factor that depends on the amount of acceptor fluorophores in the different samples. Importantly, the amount of acceptor is directly proportional to the intensities in spectra C', D', and E', where the donor and the FRET signals do not contribute at all. Thus, the contribution from direct excitation of acceptor in spectra C and D can be subtracted as shown in Equation 3

$$\begin{cases} F = C - E \times \dfrac{C'_{\mathrm{max}}}{E'_{\mathrm{max}}} \\ G = D - E \times \dfrac{D'_{\mathrm{max}}}{E'_{\mathrm{max}}} \end{cases} \quad \text{(Eq. 3)}$$

where "max" is defined as the intensity at the acceptor emission peak. The wavelength used to determine this value is 603 nm.

If the intensity of the acceptor changes in response to the drug, the emission peaks for spectra C' and D' will be different as shown in Equation 4.

$$\text{drug response} = \frac{D'_{\mathrm{max}}}{C'_{\mathrm{max}}} \quad \text{(Eq. 4)}$$

This change in intensity will also modify the signal obtained when using ExcD, in spectrum G. For instance, if the drug response is 2 in spectrum D', then the acceptor signal in spectrum G should actually be divided by 2 to have only the changes due to FRET (note that in our experiments, the responses were actually in the order of 1–3%). More generally, the acceptor signal in spectrum G should be corrected for FRET-independent drug response using the following correction factor as shown in Equation 5.

$$\text{correction factor} = 1 - \frac{C'_{max}}{D'_{max}} \quad \text{(Eq. 5)}$$

Because only the acceptor signal is affected, this correction factor should only be applied to the contribution of the acceptor in the total spectrum, which is a mix of donor and acceptor signals. The acceptor signal can be extracted using spectrum *E* and properly scaling it as was done above to obtain spectra *F* and *G* as shown in Equation 6.

$$\text{acceptor signal in spectrum } G = E \times \frac{G_{max}}{E_{max}} \quad \text{(Eq. 6)}$$

Thus, the final corrected spectrum where the FRET-independent response to drug has been subtracted is as shown in Equation 7.

$$H = G - \left(E \times \frac{G_{max}}{E_{max}}\right) \times \left(1 - \frac{C'_{max}}{D'_{max}}\right) \quad \text{(Eq. 7)}$$

Finally, spectra are normalized to keep the area under the curve constant, which also removed the contribution from any drug-induced fluorescent intensity change of the donor. As shown in Equation 8, the proximity ratio is then

$$\text{Proximity ratio} = \frac{I_A}{I_A + I_D} \quad \text{(Eq. 8)}$$

where I_D and I_A are the intensities of the donor and acceptor peaks, respectively.

When comparing the responses to drugs we used the proximity ratio. The drug response is calculated as the change in proximity ratio between spectrum *F* and spectrum *H*.

To be able to accurately calculate the distances between the fluorescent probes using the Förster theory, the proximity ratio needs to be corrected to give the FRET efficiency (18) as shown in Equation 9.

$$\text{FRET efficiency} = \frac{I_A}{I_A + \gamma I_D} \quad \text{(Eq. 9)}$$

In Equation 10, the correction factor γ is defined as

$$\gamma = \frac{\eta_A \Phi_A}{\eta_D \Phi_D} \quad \text{(Eq. 10)}$$

where η_D and η_A are the collection efficiencies of donor and acceptor signals and Φ_A and Φ_D are the fluorescence quantum yields of the donor and acceptor, respectively. We assume η_A/η_D to be 1 to obtain Equation 11.

$$\text{FRET efficiency} = \frac{I_A}{I_A + (\Phi_A/\Phi_D) I_D} \quad \text{(Eq. 11)}$$

Φ_A and Φ_D were measured by using the following relation (19) as shown in Equation 12

$$\Phi_X = \Phi_{st.} \times \frac{F_x}{F_{st.}} \times \frac{OD_{st.}}{OD_x} \quad \text{(Eq. 12)}$$

where subscripts st. and x refer to the standard and unknown solutions, respectively. *F* is the relative integrated fluorescence intensity, and *OD* is the optical density at the exciting wavelength. Rhodamine 6G was chosen as the standard (quantum yield equal to 0.90 in water) (20). Emission spectra were obtained at 25 °C using 490 nm excitation while collecting fluorescence from 496 to 800 nm. The signal from buffer solution was subtracted from each sample and from the standard before integration.

Determination of R_o

The R_0 values for the FlAsH-Alexa 568 FRET pair were calculated as shown in Equation 13 using the relationship

$$R_0 = (9.765 \times 10^3)(J(\lambda) \times \kappa^2 \times \Phi_D \times n^{-4})^{1/6} \text{ (in } \textit{panel A}) \quad \text{(Eq. 13)}$$

where κ^2 is the orientation factor (assumed to be equal to 2/3), *n* is the refractive index (equal to 1.3), Φ_D is the quantum yield of the donor, and $J(\lambda)$ is the spectral overlap integral between the emission spectrum of β_2-AR-FlAsH and the absorption spectrum of β_2-AR-Alexa 568 (in $cm^3 \cdot M^{-1}$).

Anisotropy of Bound Fluorophores

The anisotropy was determined according to Equation 14

$$r = \frac{I// - GI\perp}{I// + 2GI\perp} \quad \text{(Eq. 14)}$$

where $I//$ and $I\perp$ are the fluorescence intensities measured for parallel and perpendicular components relative to the polarized excitation and *G* the collection efficiencies of parallel and perpendicular signals.

We assumed the collection efficiencies of parallel and perpendicular signals to be the same ($G = 1$) to obtain Equation 15.

$$r = \frac{I// - I\perp}{I// + 2I\perp} \quad \text{(Eq. 15)}$$

Intensities were acquired at the maximum emission wavelength of each fluorophore over a 60-s time period and subsequently averaged. Samples were excited at the wavelengths described above. For determining any potential drug-induced changes in the anisotropy, samples were mixed and incubated for 15 min at room temperature with the concentration of drug described above.

RESULTS

Site-specific Labeling of the β_2-AR with FlAsH and Alexa Fluor 568 to Monitor the Distance between TM6 and the C Terminus by FRET—We generated a modified β_2-AR with a single FRET acceptor site at the cytoplasmic end of TM6 and two different FRET donor sites in the C terminus (Fig. 1). We started with a modified β_2-AR where 4 of the 13 endogenous cysteines (Cys-77, Cys-327, Cys-378, and Cys-406) were mutated to alanine, valine, or serine (β_2-AR-Δ4) (16). 5 of the 9 remaining cysteines are not available for derivatization because of palmitoylation (Cys-341) (21) or disulfide bond formation (Cys-106, Cys-184, Cys-190, and Cys-191) (22). 3 remaining cysteines, Cys-116, Cys-125, and Cys-285, are poorly labeled with maleimide reagents. This leaves Cys-265 at the cytoplas-

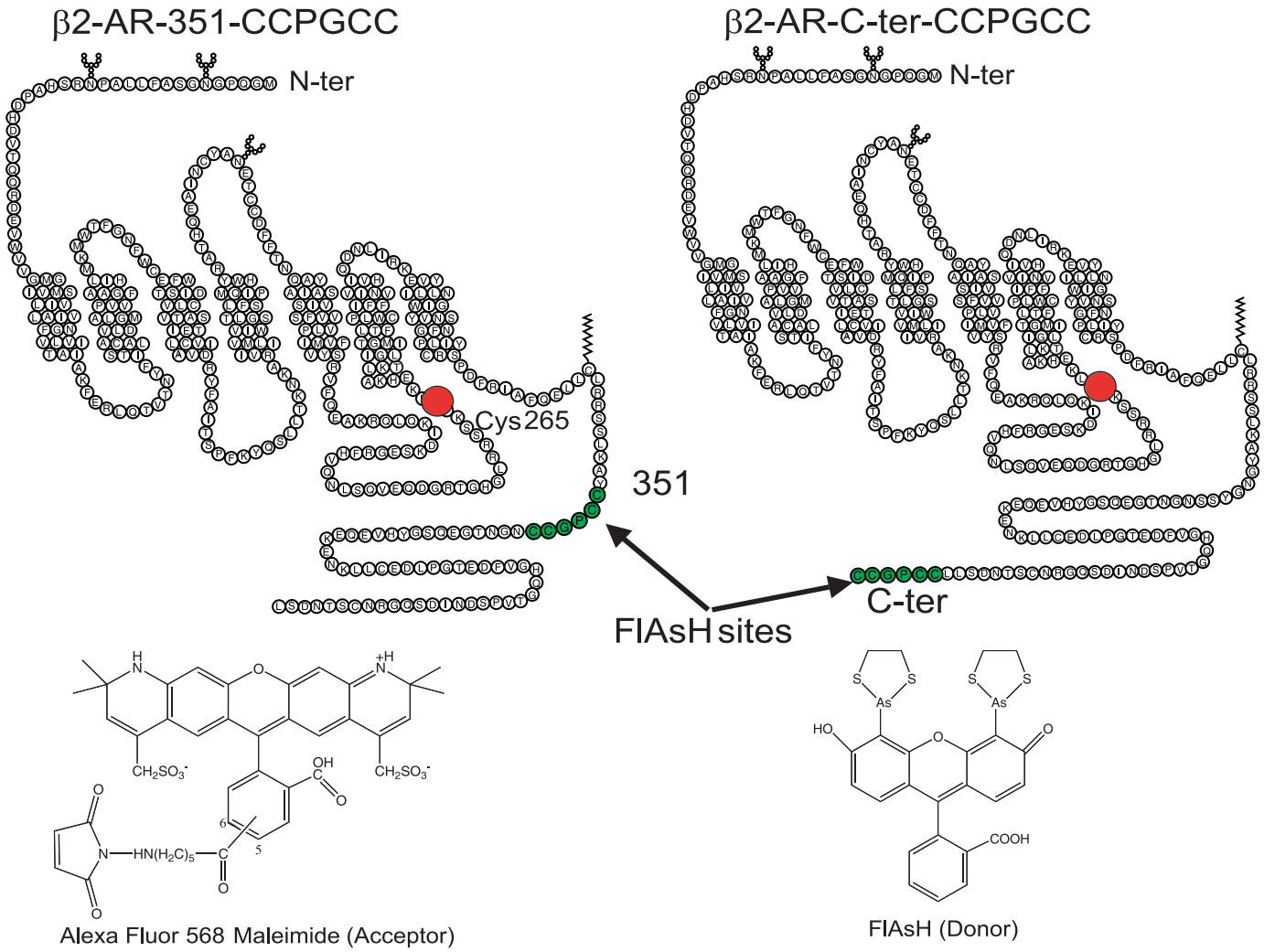

FIGURE 1. **Engineered β_2-ARs and fluorophores used in this study.** The FlAsH site (*CCPGCC*) was introduced in two alternate regions of the C-terminal domain of β_2-ARs. One starts at position 351 and is named β_2-AR-351-CCPGCC (*left*). The other was added to the C terminus of the receptor (β_2-AR-C-ter-CCPGCC, *right*). Fluorophores used in this study are FlAsH (the donor that reacts with CCPGCC) and Alexa Fluor 568 maleimide (the acceptor that reacts with cysteine 265).

mic end of TM6 as the only remaining maleimide-reactive cysteine. This site was used for attachment of the FRET acceptor Alexa 568 maleimide.

For the C-terminal FRET donor sites, we used the fluorophore 4′,5′-bis(1,2,3-dithioarsolan-2-yl)-fluorescein, also called FlAsH, commercially known as Lumio Green labeling reagent (see Fig. 1). This fluorophore binds specifically to a CCPGCC motif (FlAsH site) (23).

The first FlAsH site was introduced by replacing residues Gly-351-Ser-356, located 10 residues after the palmitoylation site (β_2-AR-351-CCPGCC), and the other was introduced following the last amino acid at the C terminus (β_2-AR-C-ter-CCPGCC) (Fig. 1, *green circles*).

As shown in Fig. 2*A*, when FlAsH was incubated overnight with the purified β_2-AR-351-CCPGCC, almost no labeling occurred. This result is consistent with the requirement for a reducing agent like TCEP in the labeling reaction and with the fact that FlAsH is not able to react with sulfhydryls such as Cys-265 (24).

The results, presented in Fig. 2*A*, reveal that the addition of 10 μM TCEP significantly enhanced the receptor labeling. Maximal labeling was obtained using 100 μM TCEP and 3 equivalents of FlAsH overnight at 16 °C. Higher concentrations of TCEP (1 mM) and FlAsH did not further increase labeling. It should be noted that 100 μM TCEP does not reduce critical disulfides necessary for maintaining β_2-AR structure. The same results were observed for the β_2-AR-C-ter construct and the level of FlAsH labeling was similar (not shown). Hence, in all our experiments, we performed FlAsH labeling in the presence of 100 μM TCEP and 3 equivalents of free dye overnight at 16 °C. The labeled receptors were also characterized by SDS-PAGE. The gel (Fig. 2*B*) shows a fluorescent band corresponding to the molecular mass of the β_2-AR for both constructs, confirming the reactivity of the CCPGCC motif. It is also interesting to note that SDS and reducing agent failed to dissociate the fluorescent labels.

It is important to note that under the same conditions we did not observe any FlAsH labeling of a β_2-AR lacking the CCPGCC motif (Fig. 2*A*), indicating that the remaining cysteines in the receptor are not reactive toward the FlAsH compound. Moreover, under the conditions used, Cys-265 is still

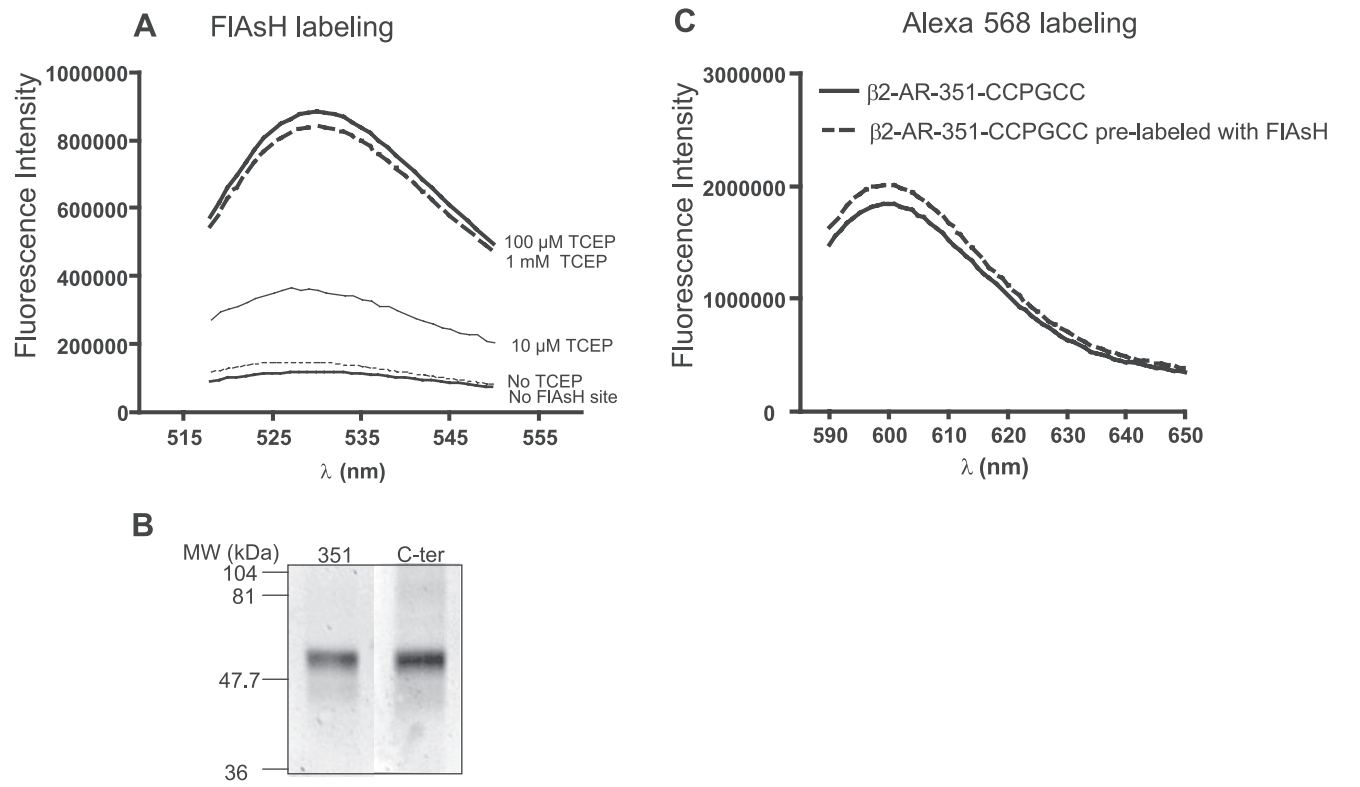

FIGURE 2. **FlAsH and Alexa Fluor 568 labeling of β_2-ARs.** *A*, FlAsH labeling of β_2-ARs. Purified receptors were incubated as described under "Experimental Procedures" in the presence of 3 equivalents of FlAsH and the indicated amount of TCEP. For the receptor lacking FlAsH sites, 100 μM TCEP was used. Emission spectra were scanned using 15 nM desalted receptor. The data represent the average of triplicate determinations and are representative of three independent sets of labeling reactions made on the same receptor preparation. *B*, SDS-PAGE of FlAsH-labeled receptor. β_2-AR-351-CCPGCC (30 pmol) and β_2-AR-C-ter-CCPGCC (40 pmol) were resolved on a 12% SDS-PAGE in denaturing and reducing conditions. Fluorescence of the gels was acquired using a Fluorchem™ 8800 (fluorescein isothiocyanate filter). *C*, Alexa Fluor 568 labeling of β_2-ARs. β_2-AR-351-CCPGCC prelabeled or not with FlAsH was incubated with 1.1 equivalents of Alexa Fluor 568 maleimide for 10 min at 4 °C. Emission scans were acquired using 15 nM desalted receptor. The data represent the average of triplicate determinations and are representative of three independent sets of labeling reactions made on the same receptor preparation.

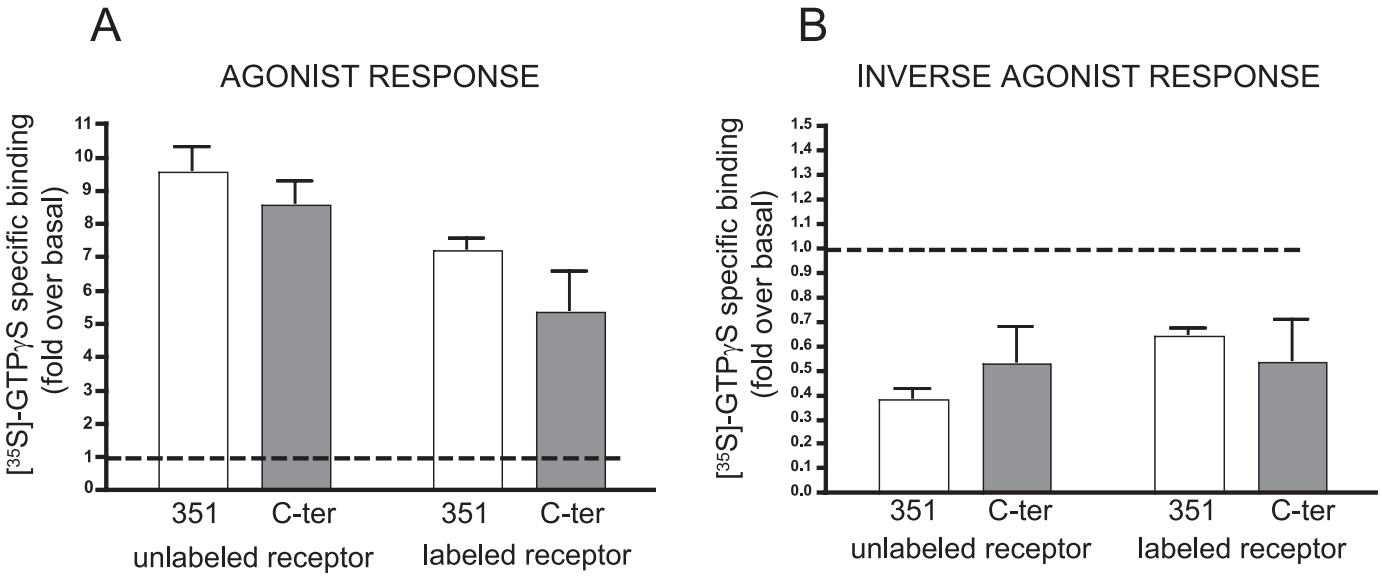

FIGURE 3. **Ligand-induced [^{35}S]GTPγS binding to purified Tet-Gαs protein reconstituted with unlabeled and double-labeled β_2-AR receptors.** Reconstitution and [^{35}S]GTPγS binding were performed as described under "Experimental Procedures." [^{35}S]GTPγS-specific binding induced by 100 μM isoproterenol (*panel A, Agonist response*) or by 10 μM ICI118,551 (*panel B, Inverse agonist response*) is represented as fold over basal for unlabeled and labeled β_2-AR-351-CCPGCC and β_2-AR-C-ter-CCPGCC constructs. The data for each panel represent the mean ± S.E. of two independent experiments performed in triplicate.

accessible to thiol reactive probes as revealed by the efficient Alexa Fluor 568 labeling of β_2-AR-351-CCPGCC prelabeled with FlAsH (Fig. 2*C*). The β2-AR-C-ter-CCPGCC construct gave similar results (Fig. 4*A*). The stoichiometry of FlAsH labeling ranged from 0.8 to 1 mol of dye/mol of receptor, and the acceptor/donor labeling ratio ranged from 1.0 to 1.3 ("Experimental Procedures"). Taken together, these results demonstrate that the FlAsH sites and Cys-265 are selectively labeled

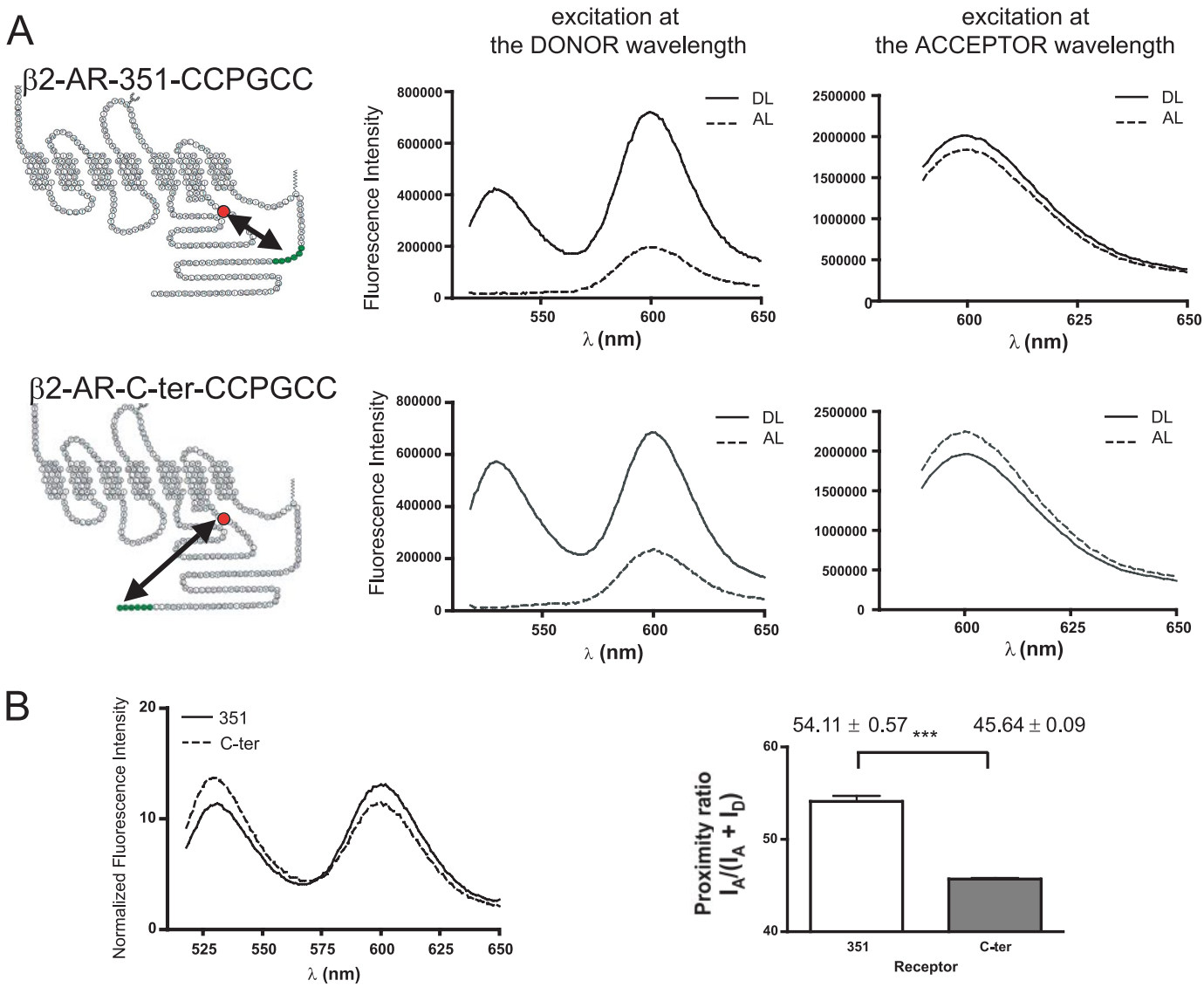

FIGURE 4. **Proximity ratio between FlAsH and Alexa Fluor 568 for β_2-AR-351-CCPGCC and β_2-AR-C-ter-CCPGCC receptors.** *A*, characteristic spectra used for FRET calculations. Both constructs were labeled as described under "Experimental Procedures." Emission scans were acquired using 15 nM desalted double-labeled (*DL*, *solid line*) receptor or receptor labeled only with the Alexa Fluor 568 (*AL*, *dotted line*). Emission scans were obtained for excitation at the donor wavelength (FlAsH, 508 nm) and at the acceptor wavelength (Alexa Fluor 568, 578 nm). The spectra represent the average of triplicate determinations and are representative of three independent sets of labeling reactions made on the same receptor preparation. *B*, normalized spectra from *panel A* and proximity ratios. Averaged spectra from triplicate determinations for β_2-AR-351-CCPGCC (*351*, *solid line*) and β_2-AR-C-ter-CCPGCC (*C-ter*, *dotted line*) were normalized as described under "Experimental Procedures." Proximity ratios (*right*) were calculated and plotted as the mean ± S.E. of three independent experiments performed in triplicate.

with a donor and an acceptor, respectively, allowing us to use FRET to monitor changes in distance between these sites.

Functional Coupling of Labeled β_2-AR to G Protein—The β_2-ARΔ4 receptor has been previously characterized and retains normal function in both ligand binding and G protein-coupling assays (16). To show that the introduction of the CCPGCC motifs does not modify receptor-G protein coupling, we measured the ligand-induced [^{35}S]GTPγS binding to purified Tet-Gαs protein reconstituted with purified receptor as previously described (17). The agonist responses for both constructs were indistinguishable from the wild-type receptor (the wild-type receptor gives routinely a 10-fold increase over basal [^{35}S]GTPγS-specific binding, not shown). As shown in Fig. 3, unlabeled reconstituted β_2-AR-351-CCPGCC and β_2-AR-C-ter-CCPGCC gave a similar response after agonist (9.5 ± 0.7- and 8.6 ± 0.7-fold over basal, respectively) or inverse agonist (0.38 ± 0.04- and 0.53 ± 0.145-fold over basal) treatment (Fig. 3, *A* and *B*).

To demonstrate that receptor labeling with the FRET probes does not modify receptor function, we performed the same experiments with double-labeled receptors. We found that labeling results in a reduction of the ligand-induced [^{35}S]GTPγS binding to purified Tet-Gαs protein (Fig. 3, *A* and *B*); nevertheless, the labeled constructs coupled efficiently and both agonist and inverse agonist effects were observed.

Determination of FRET Efficiency for β_2-AR-351-CCPGCC and β_2-AR-C-ter-CCPGCC Constructs—Purified receptors were labeled with donor and acceptor fluorophores as described above (Fig. 4*A*, *top*). Steps taken for data analysis of FRET levels in the double-labeled (*DL*) receptors are illustrated

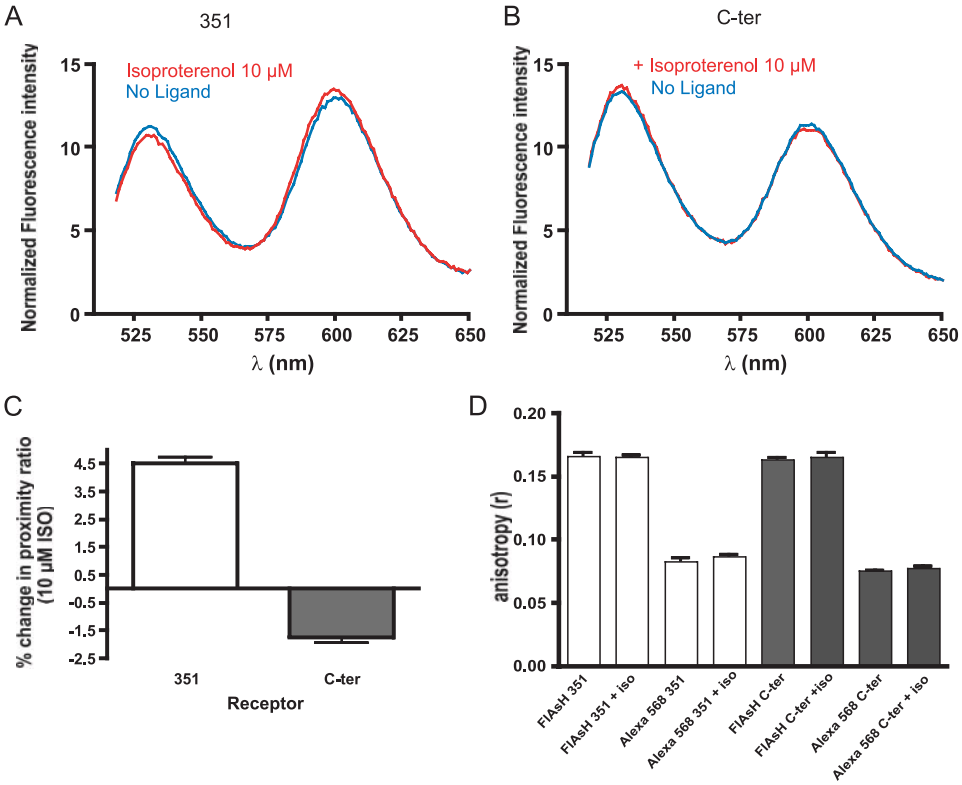

FIGURE 5. **Effects of isoproterenol on proximity ratio and anisotropy of labeled β_2-AR receptors.** β_2-AR-351-CCPGCC (*A*) or β_2-AR-C-ter-CCPGCC (*B*) were incubated for 15 min with (*red line*) or without (*blue line*) 10 μM isoproterenol. Spectra represent the average of triplicate determinations. *Panel C* represents the percentage change in proximity ratio induced by 10 μM isoproterenol for both constructs calculated from three independent experiments performed in triplicate with two different receptor preparations. *D*, anisotropy of bound fluorophores on β_2-AR-351-CCPGCC (*351*) or β_2-AR-C-ter-CCPGCC (*C-ter*). Double-labeled receptor (15 nM) was incubated for 15 min with or without 10 μM isoproterenol. Anisotropy (*r*) was calculated as described under "Experimental Procedures" after acquiring fluorescence intensities at the maximum emission wavelength of each fluorophore over a 60-s time period. Data are the mean ± S.E. of two independent experiments performed in triplicate.

in Fig. 4*A*. For all DL receptors, we measured two emission spectra, using the excitation wavelengths for the donor (FlAsH) and for the acceptor (Alexa Fluor 568). As controls, the emission spectra of receptors labeled only with Alexa Fluor 568 (*AL*) were also measured. When the receptors are labeled only with Alexa Fluor 568 on Cys-265, excitation at 578 nm results in a strong signal corresponding to Alexa Fluor 568 emission, with a maximum around 600 nm (Fig. 4*A*). Excitation at the excitation maximum for FlAsH (508 nm) resulted in small emission in the Alexa Fluor 568 channel, which represents ~10% of the full signal obtained when exciting directly at the Alexa Fluor 568 excitation maximum (Fig. 4*A*). Thus, when the receptor is labeled with both probes, the excitation at the FlAsH peak results in a mixture of three signals: FlAsH emission, Alexa Fluor 568 emission resulting from FRET, and some Alexa Fluor 568 emission resulting from direct excitation at 508 nm (Fig. 4*A*, *excitation at the donor wavelength DL*). The latter bleedthrough fluorescence is subtracted using the spectra for Alexa Fluor 568 single-labeled receptor as a template (see "Experimental Procedures"), and after normalization we obtained the spectra shown in Fig. 4*B*. The proximity ratios were calculated for both constructs (Fig. 4*B*, *bar graph*). The FlAsH/Alexa Fluor 568 proximity ratio is significantly higher for β_2-AR-351-CCPGCC than for β_2-AR-C-ter-CCPGCC (54.11 ± 0.57 *versus* 45.64 ± 0.09 in %).

To calculate FRET efficiencies, we determined the fluorescence quantum yield of FlAsH and Alexa Fluor 568 bound to the receptor as described under "Experimental Procedures." We found that the FlAsH quantum yields were similar when conjugated to either β_2-AR-351-CCPGCC or β_2-AR-C-ter-CCPGCC (0.42 ± 0.03 *versus* 0.44 ± 0.05). The Alexa Fluor 568 quantum yields were also similar for both constructs (0.121 ± 0.016 *versus* 0.114 ± 0.013). Using these values we determined the basal FRET efficiency to be 83.35% for β_2-AR-351-CCPGCC and 77.02% for β_2-AR-C-ter-CCPGCC. The R_0 value for the FRET pair used in this study (FlAsH-Alexa 568) was found to be 75 Å. From FRET efficiencies and R_0 we calculated $R_{Proximal}$ to be 56.96 ± 0.17 Å and R_{Distal} to be 62.05 ± 0.04 Å.

Isoproterenol-induced Changes in Proximity Ratio—To look at possible structural changes in the C-terminal domain of receptors upon ligand binding, we sought to determine whether agonist treatment could modify the FRET signals. As shown in Fig. 5, *A* and *B*, when isoproterenol was added to purified receptors we observed changes in fluorescence intensity for the donor and acceptor peaks in the corrected spectra, indicative of a change in proximity ratio. Calculated proximity ratio for the β_2-AR-351-CCPGCC construct significantly increased from 55.36 ± 0.11 to 57.93 ± 0.17% (Fig. 5*A*). In contrast to the β_2-AR-351-CCPGCC, isoproterenol treatment of the β_2-AR-C-ter-FlAsH construct led to a decrease in the proximity ratio from 45.60 ± 0.05 to 44.63 ± 0.08.

The percentage change in proximity ratio for both constructs, calculated from at least three independent experiments performed in triplicate, is shown in Fig. 5*C* and clearly demonstrates a difference between the two receptor constructs used in this study. Agonist treatment led to a change in proximity ratio of 4.5 ± 0.2% for the β_2-AR-351-CCPGCC and −1.74 ± 0.19% for the β_2-AR-C-ter-CCPGCC.

To rule out the possibility that these results were caused by changes in the mobility or orientation of the fluorophores, we determined the anisotropy of fluorophores attached to the receptors before or after treatment with isoproterenol. Results showed that bound Alexa Fluor 568 has a high degree of rotational freedom (small anisotropy) that was not altered by isoproterenol treatment (Fig. 5*D*). The anisotropy of bound FlAsH was significantly higher than the anisotropy of bound Alexa Fluor 568; however, there was no significant change upon isoproterenol treatment (Fig. 5*D*).

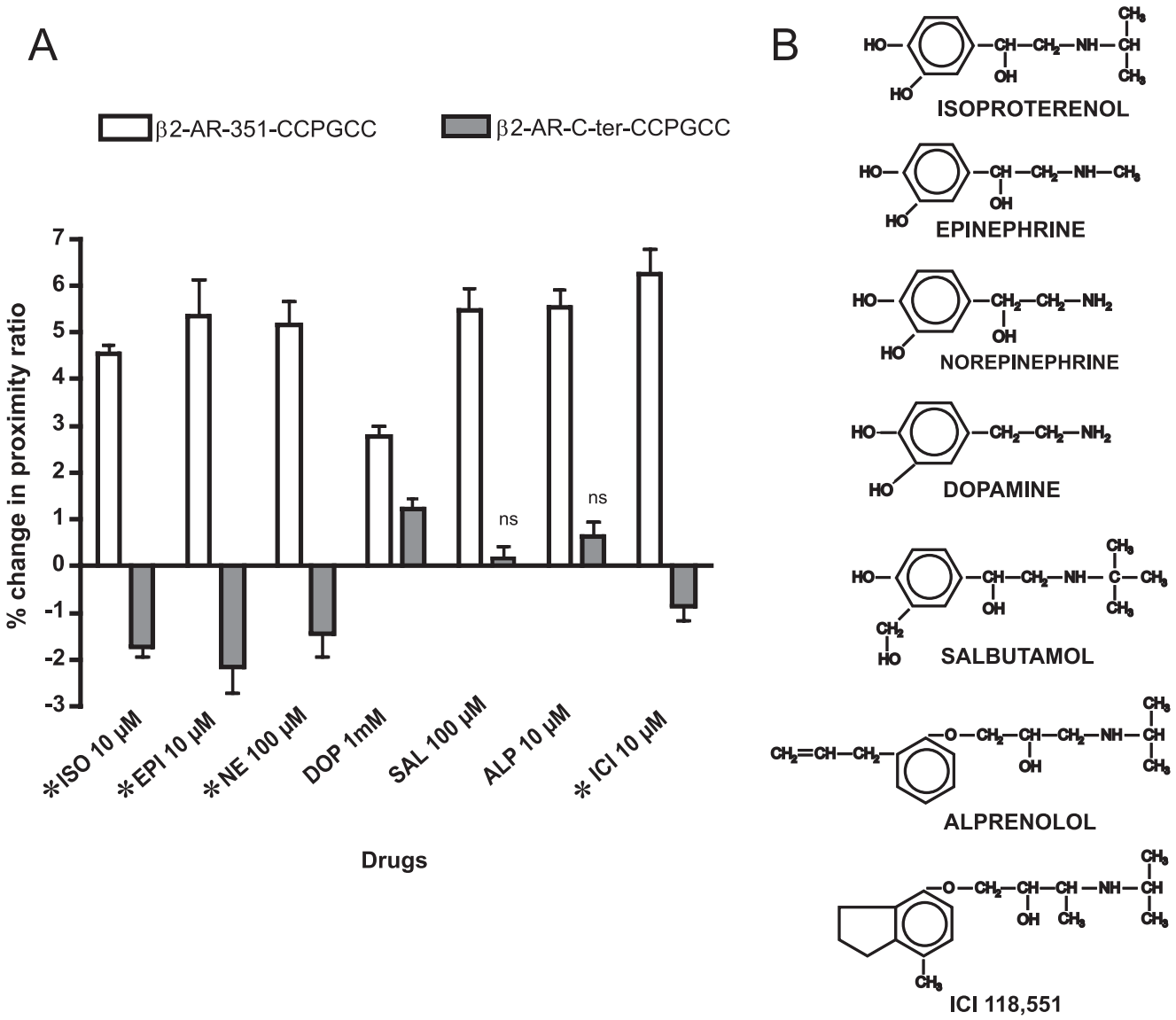

FIGURE 6. **Changes in proximity ratio after drug treatments.** *A*, β_2-AR-351-CCPGCC or β_2-AR-C-ter-CCPGCC were incubated for 15 min with or without the indicated amount of drugs. Results are the percentage change in proximity ratio calculated from three independent experiments performed in triplicate with two different receptor preparations. Except for those noted *ns* (non-significant), all values are significantly different ($p < 0.05$) from the no-drug control as determined by Student's *t* tests. Stars (*) denote the agonist nature of ligands for the MAPK pathway. *B*, structures of ligands used in this study.

Effect of Structurally and Functionally Different Ligands on Proximity Ratio of β_2-AR Receptors—We then investigated the effects of functionally different ligands on the proximity ratio for both receptor constructs. Our ligands included the agonists isoproterenol, epinephrine, and norepinephrine, the partial agonists dopamine and salbutamol, the antagonist alprenolol, and the inverse agonist ICI-118,551 (Fig. 6*B*). All ligands were used at saturating concentrations. Fig. 6*A* shows the ligand-specific changes in proximity ratio. Remarkably, for the β_2-AR-351-CCPGCC construct, all the ligands triggered a significant increase in proximity ratio ranging from 2.76 to 6.24%.

In agreement with the isoproterenol response, treatment of the β_2-AR-C-ter-CCPGCC with catecholamine agonists epinephrine and norepinephrine induced a decrease in proximity ratio (-2.15 ± 0.57 and -1.43 ± 0.51% change respectively). By contrast, the catecholamine partial agonist dopamine induced an increase in the FRET efficiency by 1.23 ± 0.21%. Salbutamol and alprenolol did not induce any significant change in FRET as compared with untreated β2-AR-C-ter-CCPGCC receptor. Finally, we observed that the inverse agonist ICI-118,551 induced a significant decrease in FRET signals by -0.88 ± 0.25%.

DISCUSSION

Little is known about the structure of the C termini of GPCRs. This domain is involved in interactions with GRKs and arrestins as well as PDZ domains of other signaling and regulatory proteins. We used FRET to gain insight into both the structure and ligand-induced conformational changes of the β_2-AR C terminus.

FRET can be used as a molecular ruler to measure distances between two protein domains if each domain can be selectively labeled with donor and acceptor fluorophores. We used FlAsH sites (23) for site-specific labeling with a donor fluorophore. The arsenical FlAsH compounds bind to a tetracysteine motif

(CCPGCC) that can be introduced into specific sites within the protein of interest, thus providing a labeling chemistry orthogonal to single-cysteine labeling at cysteine 265 (25).

We engineered β_2-AR receptors containing a CCPGCC motif in either the proximal C terminus, located 10 amino acids from the palmitoylation site at the end of the 8th helix (β_2-AR-351-CCPGCC), or the extreme C terminus (β_2-AR-C-ter-CCPGCC). The proximal site lies within a proteolytic fragment previously shown by mass spectrometry to be phosphorylated upon agonist activation of β_2-AR expressed in human embryonic kidney 293 cells (26). We showed that FlAsH (donor fluorophore) efficiently labels the C-terminal CCPGCC sites. Cysteine 265 is not labeled by FlAsH and thus can be specifically labeled with Alexa Fluor 568 maleimide in a separate reaction (see Fig. 2*A*). This labeling strategy allowed us to monitor movement of the C terminus of the β_2-AR relative to the cytoplasmic end of TM6 using FRET. Cysteine 265 was chosen as the reference site because previous studies have demonstrated that it is highly reactive toward maleimides, and we observed that this domain undergoes conformational changes in response to agonist binding (7, 27). We confirmed that double-labeled receptors are able to couple to G proteins, demonstrating that our FRET measurements reflect conformational changes in a functional receptor.

The C Terminus of the β_2-AR Is in an Extended Conformation—The C terminus of rhodopsin has been determined by x-ray crystallography. Although the b-factors for this domain are relatively high, the domain is structured and compactly folded over the 8th helix and first intracellular loop (15). We were therefore surprised to find that the C terminus of the β_2-AR appears to be in an extended and possibly unstructured conformation. The R_0 value for the FRET pair used in this study (FlAsH-Alexa 568) was found to be 75 Å. Because FRET efficiency is directly related to the distance between the two fluorophores, our data indicate that $R_{\text{Proximal}} = 57$ Å and $R_{\text{Distal}} = 62$ Å. These values represent the average distance between the donor and acceptor fluorophores. These distances are relatively large, indicating that the C terminus is in an extended conformation. In contrast, the distance in rhodopsin homologous to R_{Proximal} is only 17 Å (15). To determine the average distance expected in an unstructured C terminus, we measured the FRET efficiency for β_2-AR-C-ter-CCPGCC in 8 M urea. We found that the FRET efficiency decreased by only 7.6%, corresponding to a difference of ~3 Å. Thus, in the native β_2-AR, the average distance between Cys-265 and the distal C terminus is similar to the distance observed in β_2-AR denatured with urea.

Anisotropy measurements also support a more flexible C terminus. FlAsH fluorophores are bound to the peptide backbone through four covalent bonds producing a rigid link with the peptide backbone (25). Therefore the anisotropy of the FlAsH probes reflects the dynamics of the protein domain. Anisotropy values for FlAsH probes bound to both proximal and distal sites were relatively low ($r = 0.17$, Fig. 5). Higher values would be expected for FlAsH probes bound to a rigid domain of a 50-kDa protein imbedded in a detergent micelle (28). Therefore, the anisotropy data are consistent with the FRET data, suggesting that the C terminus of the β_2-AR is relatively flexible.

There is a growing awareness that many proteins have intrinsically unstructured domains and that the lack of structure plays an important role in protein function (29, 30). These unstructured domains serve as binding sites for interacting proteins. The extended, flexible sequence facilitates rapid protein-protein interactions and the formation of multiprotein complexes (29, 30). The unstructured nature of the β_2-AR C terminus may play a role in functional interactions with cytosolic proteins such as GRKs, arrestins, *N*-ethylmaleimide-sensitive factor, and PDZ domain-containing proteins such as NHERF/EBP50. Although the unstructured nature of the C terminus may be important for receptor function, it may be an impediment to obtaining diffraction quality crystals for high resolution structure determination.

Ligand-specific Changes in FRET Efficiency—Interactions between the C terminus of the β_2-AR and GRKs and arrestins are regulated by ligands. Therefore, we looked for ligand-induced changes in the distance between the cytoplasmic end of TM6 and the C terminus. TM6 forms part of the agonist binding pocket, and the cytoplasmic end of TM6 undergoes conformational changes following agonist binding (9, 27). We did not obtain evidence for large structural changes in the C terminus upon agonist binding. Nevertheless, the results shown in Fig. 5 indicate that isoproterenol binding is accompanied by a relatively small but significant structural change where the distance between the proximal C terminus and Cys-265 is reduced, while the distance between the distal C terminus and Cys-265 is increased. It is unlikely that these effects are caused by a change in fluorophore orientation, given that the anisotropies of bound FlAsH and Alexa Fluor 568 are (i) relatively low and (ii) unaffected by isoproterenol.

We also investigated conformational changes induced by structurally and functionally different ligands. Remarkably, for the β_2-AR-351-CCPGCC construct, all tested ligands gave FRET efficiency changes of similar direction and magnitude. By contrast, we observed ligand-specific responses for the β2-AR-C-ter-CCPGCC construct. Binding of a neutral antagonist (alprenolol) and an inverse agonist (ICI-118,551) induces different structural changes. Our results also indicate a difference in the orientation of the extreme C terminus relative to cysteine 265 in response to catechol agonists (decrease in FRET efficiency for isoproterenol, epinephrine, and norepinephrine) and a non-catechol partial agonist (no change in FRET efficiency for salbutamol). These results are in agreement with previous data showing that structurally similar ligands can induce distinguishable active states (8). Of interest, the response to the inverse agonist ICI118,551 was similar to that for catechol agonists (FRET efficiency increase for the proximal C terminus and decrease for the C terminus, Fig. 6*A*, *). These results provide a structural basis for a common functional property associated with these ligands: the ability to stimulate the MAPK pathway (14). The C-terminal domain is critical for this signaling function (14).

Conformational changes involving the C termini of GPCRs have been demonstrated using FRET in living cells (31). In this study, cyan fluorescent protein (the donor) added to the C terminus of the A_{2A} adenosine receptor and a FlAsH binding site (acceptor) was engineered into the third intracellular loop. In

this case, agonist binding led to a 10% change in FRET efficiency. This appears as a larger change than observed in our studies; however, based on the Förster theory, the calculated amplitude of this conformational switch ranges from 1 to 2 Å (considering 40 Å $< R_0 <$ 75 Å). These values are even smaller for the other FRET pair cyan fluorescent protein/yellow fluorescent protein ($R_0 \sim 50$ Å) introduced in the same positions in the A_{2A} adenosine receptor (0.4 Å, with a 55% FRET efficiency and a 2% change after agonist treatment) (31). These values are compatible with our results where changes in FRET efficiency of 6% correspond to a change in distance of ~2 Å when the R_0 for the FRET pair is 75 Å. In both cases, these results support the conclusion that the distal C-terminal domain is moving away from the core structure of the receptor upon agonist binding. One could propose that this movement facilitates interactions with regulatory proteins such as GRKs and arrestins.

In conclusion, these FRET studies provide evidence that the C terminus of the β_2-AR is an extended, relatively flexible, and possibly disordered structure. Nevertheless, ligand-specific changes can be detected in the distance between the C terminus and the cytoplasmic end of TM6. Of interest, we observed that catecholamine agonists induced changes in FRET similar to those induced by an inverse agonist. This may reflect a conformational change necessary for arrestin-dependent activation of the MAPK pathway.

Acknowledgments—We thank Dr. Charles Parnot for help with the analysis of FRET data and Mike Bokoch and Dr. Xavier Deupi for critical reading of the manuscript.

REFERENCES

1. Ji, T. H., Grossmann, M., and Ji, I. (1998) *J. Biol. Chem.* **273,** 17299–17302
2. Ballesteros, J. A., Shi, L., and Javitch, J. A. (2001) *Mol. Pharmacol.* **60,** 1–19
3. Farrens, D. L., Altenbach, C., Yang, K., Hubbell, W. L., and Khorana, H. G. (1996) *Science* **274,** 768–770
4. Altenbach, C., Cai, K., Khorana, H. G., and Hubbell, W. L. (1999) *Biochemistry* **38,** 7931–7937
5. Cai, K., Klein-Seetharaman, J., Farrens, D., Zhang, C., Altenbach, C., Hubbell, W. L., and Khorana, H. G. (1999) *Biochemistry* **38,** 7925–7930
6. Altenbach, C., Klein-Seetharaman, J., Cai, K., Khorana, H. G., and Hubbell, W. L. (2001) *Biochemistry* **40,** 15493–15500
7. Swaminath, G., Xiang, Y., Lee, T. W., Steenhuis, J., Parnot, C., and Kobilka, B. K. (2004) *J. Biol. Chem.* **279,** 686–691
8. Ghanouni, P., Gryczynski, Z., Steenhuis, J. J., Lee, T. W., Farrens, D. L., Lakowicz, J. R., and Kobilka, B. K. (2001) *J. Biol. Chem.* **276,** 24433–24436
9. Ghanouni, P., Steenhuis, J. J., Farrens, D. L., and Kobilka, B. K. (2001) *Proc. Natl. Acad. Sci. U. S. A.* **98,** 5997–6002
10. Benovic, J. L. (2002) *J. Allergy Clin. Immunol.* **110,** Suppl. 6, S229–S235
11. Reiter, E., and Lefkowitz, R. J. (2006) *Trends Endocrinol. Metab.* **17,** 159–165
12. Lefkowitz, R. J., and Shenoy, S. K. (2005) *Science* **308,** 512–517
13. Ren, X. R., Reiter, E., Ahn, S., Kim, J., Chen, W., and Lefkowitz, R. J. (2005) *Proc. Natl. Acad. Sci. U. S. A.* **102,** 1448–1453
14. Azzi, M., Charest, P. G., Angers, S., Rousseau, G., Kohout, T., Bouvier, M., and Pineyro, G. (2003) *Proc. Natl. Acad. Sci. U. S. A.* **100,** 11406–11411
15. Okada, T., Sugihara, M., Bondar, A. N., Elstner, M., Entel, P., and Buss, V. (2004) *J. Mol. Biol.* **342,** 571–583
16. Gether, U., Lin, S., Ghanouni, P., Ballesteros, J. A., Weinstein, H., and Kobilka, B. K. (1997) *EMBO J.* **16,** 6737–6747
17. Swaminath, G., Deupi, X., Lee, T. W., Zhu, W., Thian, F. S., Kobilka, T. S., and Kobilka, B. (2005) *J. Biol. Chem.* **280,** 22165–22171
18. Ha, T., Ting, A. Y., Liang, J., Caldwell, W. B., Deniz, A. A., Chemla, D. S., Schultz, P. G., and Weiss, S. (1999) *Proc. Natl. Acad. Sci. U. S. A.* **96,** 893–898
19. Chen, R. F. (1965) *Science* **150,** 1593–1595
20. Magde, D., Wong, R., and Seybold, P. G. (2002) *Photochem. Photobiol.* **75,** 327–334
21. O'Dowd, B. F., Hnatowich, M., Caron, M. G., Lefkowitz, R. J., and Bouvier, M. (1989) *J. Biol. Chem.* **264,** 7564–7569
22. Dohlman, H. G., Caron, M. G., DeBlasi, A., Frielle, T., and Lefkowitz, R. J. (1990) *Biochemistry* **29,** 2335–2342
23. Griffin, B. A., Adams, S. R., and Tsien, R. Y. (1998) *Science* **281,** 269–272
24. Griffin, B. A., Adams, S. R., Jones, J., and Tsien, R. Y. (2000) *Methods Enzymol.* **327,** 565–578
25. Adams, S. R., Campbell, R. E., Gross, L. A., Martin, B. R., Walkup, G. K., Yao, Y., Llopis, J., and Tsien, R. Y. (2002) *J. Am. Chem. Soc.* **124,** 6063–6076
26. Trester-Zedlitz, M., Burlingame, A., Kobilka, B., and von Zastrow, M. (2005) *Biochemistry* **44,** 6133–6143
27. Yao, X., Parnot, C., Deupi, X., Ratnala, V. R., Swaminath, G., Farrens, D., and Kobilka, B. (2006) *Nat. Chem. Biol.* **2,** 417–422
28. Lakowicz, J. R. (2006) *Principles of Fluorescence Spectroscopy*, 3rd Ed., Springer Science+Business Media, LLC, New York
29. Dyson, H. J., and Wright, P. E. (2005) *Nat. Rev. Mol. Cell. Biol.* **6,** 197–208
30. Tompa, P., Szasz, C., and Buday, L. (2005) *Trends Biochem. Sci.* **30,** 484–489
31. Hoffmann, C., Gaietta, G., Bunemann, M., Adams, S. R., Oberdorff-Maass, S., Behr, B., Vilardaga, J. P., Tsien, R. Y., Ellisman, M. H., and Lohse, M. J. (2005) *Nat. Methods* **2,** 171–176